SEMANTIC NAVIGATION MAPS FOR MOBILE ROBOT LOCALIZATION ON PLANETARY SURFACES

Juergen Rossmann[(1)], Gregor Jochmann[(2)], Florian Bluemel [(2)]

[(1)] Institute for Man-Machine Interaction, RWTH Aachen University, Ahornstraße 55, Aachen, Germany, Email: rossmann@mmi.rwth-aachen.de

[(2)] Department Robot Technology, RIF e.V., Josef-von-Fraunhofer-Straße 20, Dortmund, Germany, Email: [jochmann|bluemel]@rt.rif-ev.de

ABSTRACT

Exploration with autonomous mobile robots is an important means in recent space exploration missions. One key requirement imposed is the ability to localize the robots in relation to their environment and to represent this environment in an accessible way.

This paper discusses map building and localization for mobile robot exploration missions on planetary surfaces using a novel map representation we call *semantic navigation map*. We define and discuss the concept of our map representation, show how the map is generated, and explain how the localization algorithm utilizes and extends the map during the exploration phase of the mission. Finally, we demonstrate the feasibility of our concept in a virtual testbed.

1. INTRODUCTION

An important aspect of mobile robot operation on planetary surfaces is a reliable and exact localization, as it is fundamental for safe navigation and exploration.

Prior research in this area has established two major classes of the localization problem: The task of determining the robot's pose given a very poor initial estimate, or even none at all, is called *global localization*. For the *tracking problem*, a sufficiently accurate pose estimate is known and is tracked over time.

Typically, in current planetary exploration scenarios mobile robots are tele-operated or move autonomously between points of interest. Localization in this context requires a model of the robot's surroundings called the *navigation map* [1].

The related problem of generating or updating a navigation map is called *mapping*. For exploration scenarios, the approach of *simultaneous localization and mapping* (SLAM [2]) is of special interest.

Navigation maps can be classified by the represented structure as either metric or topological. Topological maps consist of distinct places that are linked by possible transitions to form a graph. In metric maps, objects in the environment have a position in continuous Cartesian space. A metric model allows transformations between map-relative and robot-relative position estimates. Typical representations are *feature maps* that store environment features along with their positions [3] and *free-space maps* that represent the robot-accessible portion of the environment [4].

Choosing a suitable map representation is not a trivial task and usually linked to choosing the localization algorithm and sensor equipment. Different classes of localization algorithms call for specific and diverse definitions of features and landmarks in a map. As a result, typical navigation maps are highly specialized and define landmarks in terms of the chosen algorithms' search domains. These maps often do not correspond to a human operator's intuitive understanding of the robot's environment.

In previous work, we presented a general localization framework for landmark-based localization [5]. The modular structure of this framework suggests a further separation of the represented map and the localization components.

This paper presents the concept of a semantic navigation map. In this metric, landmark-based map representation landmarks carry semantic information and are intuitively accessible. This high level of abstraction leads to a map concept that is suitable for a broad range of applications, and thus simplifies evaluation and comparison of localization-related algorithms. At the same time, the environment models are comprehensible and easily editable. Additionally, SLAM-based exploration results in maps that are not restricted to the problem domain of localization.

2. MAP CONCEPT

A landmark-based navigation map is composed of landmark observations that have been reduced to relevant characteristics. The chosen subset of significant features will typically depend on sensor availability and detection methods.

For a semantic navigation map, we choose landmarks to possess meaning in the intuitive, usually geographic sense. That is, we expect landmarks to be rocks, mountains or trees, rather than e.g. SIFT feature vectors specific to some implementation of a localization method. Depending on the type of landmark, an abstraction of a set of observable features is defined. The selected features often correspond to a simplified visualization of the landmark: A sphere could represent

a rock with only one feature, its radius, while rocks annotated with height and radius would imply a cylinder as visualization.

Because the notion of a landmark in the semantic map emphasizes human perception, implications with respect to localization-related algorithms have to be carefully considered. Usually some, but not all of the obvious landmark features are detectable by a specific set of sensors and suitable for a specific localization algorithm. To bridge this gap, we introduce a quality measure that expresses *relevance* and *expected observability* of a landmark with respect to specific sensors and algorithms. Map usage flexibility is maximized by storing suitable quality indicators during map generation. These are then utilized to derive the quality measure once the specific set of sensors is known.

A semantic navigation map can be based on a digital elevation model (DEM, sometimes digital terrain model DTM). While this is optional in regard to 2D localization, it greatly improves usability of the map for visualization and human orientation. In the context of mobile robot localization on planetary surfaces, navigation maps can be generated from imagery obtained during descent and landing. This initial map can later be refined by SLAM algorithms, but more importantly, may already indicate hazards that are not easily discoverable from a mobile robot's perspective.

As we are going to show in section 4, the concept supports a variety of different localization algorithms. This allows us to use such maps in a modular testbed environment where different algorithms can be used without having to modify the map representation. Further, the concept is not tied to planetary exploration applications. In section 5, we apply the same concept to localization in forest environments.

Three basic types of geological landmarks in planetary exploration are rocks, craters and mountain tops. Rocks are not only an important subject of study in ongoing missions [6] but are also essential for exact localization and tracking on a local scale. From the ground perspective of a mobile robot, rocks typically serve as clear landmarks that can be detected with a relatively wide range of algorithms and close-range sensors, including laser scanners, stereo cameras and time-of-flight cameras. While including texture and shape as features is possible, representing rocks by height and radius is usually sufficient.

Large craters can be used for entry and descent navigation [7]. In the context of a semantic navigation map, they are useful to position the map in known geographic coordinates of the planetary surface. To mobile robot navigation, medium and small craters are hazards or obstacles that are relevant to path planning [7]. Suitable features are depth and radius. Since many craters are more accurately described as ellipses, an alternative is using major and minor axis length instead of radius.

Mountain tops are prominent landmarks that can be used for global-scale localization. If suitably chosen, they are distinct features in the panoramic horizon observed by a mobile robot [9]. Depending on map usage, variations in shape and slope can be neglected, leaving summit height as defining feature.

3. MAP GENERATION

In this section, we describe how imagery recorded during descent and landing on a planetary surface generates a semantic navigation map. A surface representation is calculated and provides a frame of reference for landmark observations. The set of observations is further examined to improve quality and merge duplicates; finally, the observations are valuated and the navigation map is populated with the resulting semantic landmarks.

Typical planetary descent and landing scenarios include extensive recording of aerial imagery. As a basis for the semantic navigation map, a digital elevation model is generated. This dense surface reconstruction is calculated from monocular images and without additional knowledge of camera motion [10]. An important by-product from this method is a global coordinate system, including estimated camera poses for the images.

3.1. Landmark Detection and Positioning

Mountains are morphological features and are detected by DEM inspection. The DEM is scanned for local maxima. Low hills, flat dunes or stretched ridges are usually not clearly visible from ground perspective; to reject these, topographical prominence and isolation is calculated. Topographical prominence describes the height of a summit above the lowest contour line encircling it; topographical dominance is the distance to the nearest point of equal elevation. The expected visibility from ground perspective is directly derived from these measures.

Rocks can be detected in entry, descent and landing (EDL) imagery using shadows as indicating visual features [11]. After the segmentation of shadow regions, shadows are approximated by ellipses. With these and a known sun direction, the height and width of an alleged stone is derived.

Craters appearances and sizes depend on widely varying factors like geological age and magnitude of impact. We use an imaging based approach to detect sufficiently defined craters [7]. After edge detection, convex edges are classified as opening or closing crater edges. By considering sun direction and luminance gradients, suitable edges are paired to infer crater ellipses.

The imaging based algorithms yield 2D positions for the landmark detections, local to the respective image. Furthermore, estimated camera poses are known and the DEM provides an interpretation of the image contents as

a 3D surface. This information is used to globally position the landmark observations by perspective projection. It should be noted that this projection introduces no new errors, but is consistent with any inaccuracies in the DEM and camera pose estimates.
In the case of craters, the depth at the landform's center point can now be determined.

3.2. Cleaning and Merging

When all detections have been collected, plausibility tests are applied to clean the set containing the observed landmarks. Even some systematic errors can be caught by matching landmarks of different types.
A straightforward notion to reject some erroneous crater detections is using the depth sampled from the DEM. Clearly, no correct crater detection should have negative depth; furthermore, the ratio of diameter to depth is used to reject shallow craters.
A systematic rock detection error is induced by the basic assumption that all shadows are cast by rocks. This simplification is necessary for the chosen approach and mostly valid in the context of planetary exploration; an obvious and prominent counter example is given by crater shadows. Since craters are detected using different indicators, they can be used to correct this kind of error. The direction from rock to crater detection and the elliptic crater radius in this direction are calculated. Using these, rock observations on or close to light-facing crater edges are rejected.
Individual landmarks are typically observed in overlapping regions from different images. These observations have to be merged to arrive at uniquely represented abstract landmarks for the semantic navigation map.
Multiple observations of single landmarks have the same type and originate from different images. With this preliminary characterization, spatial proximity is used as a sufficient criterion for identification. For detections d identified as observations of a single landmark L, the detected features f are merged by weighting with the detection quality q (Figure 1).

$$L = \{d_1, d_2, \dots\} \tag{1}$$

$$d = (q, f_1, f_2, \dots) \tag{2}$$

$$f(L) = \frac{\sum_{d \in L} q(d) \cdot f(d)}{\sum_{d \in L} q(d)} \tag{3}$$

3.3. Landmark Valuation

Our localization and navigation methods benefit from a quality measure that represents estimated landmark observability. We infer this valuation from confidence in visual observation correctness and estimated merge errors. We further refine this measure by considering rover sensors and detection methods used in exploration.
For image-based landmark detections, we intuitively expect any landmark that was observed in one image to be observable in other images showing the same region with the same or better resolution. This expectation suggests a quality measure *multiplicity-based confidence* $q_{\#}$. From the images showing a landmark L, we choose i_0 to be the image covering the largest area of ground, and define

$$I = \{i \in \text{Images} \mid \text{area}(i) \leq \text{area}(i_0)\} \tag{4}$$

$$q_{\#} = \frac{\#\{i \in I \mid L \text{ detected in } i\}}{\#\{i \in I \mid i \text{ covers } L\}} \tag{5}$$

When a landmark is merged from multiple image-based

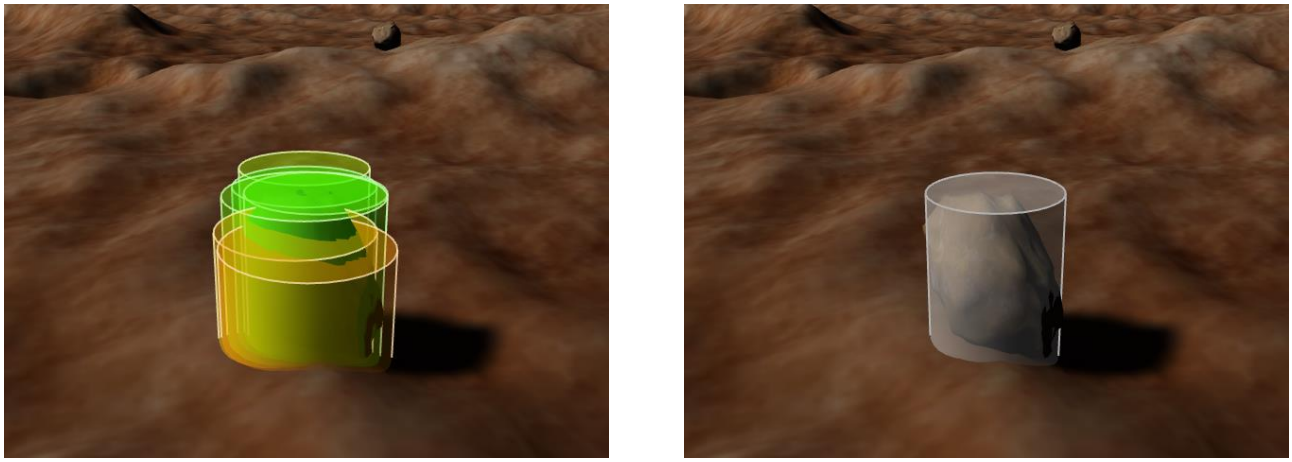

Figure 1: Merging of landmark observations. A rock was detected in multiple images and with varying confidence (left). By weighting the individual feature estimates with detection quality, a single landmark is inferred (right).

detections, low variance in the feature values can be interpreted as high confidence in observation correctness. For a feature f with mean $\bar{x}_f$ and standard deviation s_f, the coefficient of variation cv_f is estimated as

$$cv_f = \frac{s_f}{\bar{x}_f} \tag{6}$$

The coefficient of variation is 0 if all observations match exactly. On the other hand, $cv_f > 1$ implies greater deviation than mean, that is, an unusable feature value. We thus define the *variance-based confidence* q_f in an observed feature value as

$$q_f = \max\{1 - cv_f, 0\} \tag{7}$$

The quality indicators q_f and $q_\#$ are stored with the map. These indicators are generic, and thus the resulting map representation is not yet tied to a specific usage scenario. To use the map for localization or navigation purposes, the quality indicators have first to be evaluated accordingly: Some landmark features can have far greater influence on landmark observability than others, depending on available sensors. When given additional knowledge on the intended use of the semantic navigation map, it is possible to decide feature importance. Given feature weights w_f, the resulting landmark quality is

$$q = q_\# \cdot \sum_{f \in F} w_f q_f \text{ with } \sum_{f \in F} w_f = 1. \tag{8}$$

As a practical usage example for the navigation map, we studied a mobile robot that self-localizes using horizontal laser scans. Rock perceptions are deduced from the scan data and have to be matched against the navigation map. In this scenario, the quality of rock height estimates is of minor importance, while good position and diameter estimates are crucial for the correct matching of observations to landmarks.

4. MAP UTILIZATION

The map representation is a vital part of our localization framework [5]. The framework defines the interfaces of the components used to perform self-localization on mobile robots. The framework itself does not contain localization algorithms. Instead, it provides the tools to develop localization solutions for arbitrary application scenarios where using metric landmark maps is feasible.
In [5], we describe how localization with respect to metric landmark navigation maps can be divided into two major steps with clear interfaces – *landmark detection* and *localization.* The *landmark detection step* uses sensor information to generate landmark observations relative to the robots local coordinate system. *The localization step* uses these observations, the navigation map, and additional sensor data to calculate the estimated pose of the robot. The localization step is independent of the application scenario, allowing us to reuse the same methods in any scenario where landmark detectors are available. This abstraction is achieved using object-oriented design principles as described in [12].

4.1. Landmark Identification using Semantic Information

The landmark identification problem is an important element of all landmark-based localization algorithms. Landmark identification uses the local detections extracted from sensor information in the landmark detection step. For each detection $d \in D$, the localization algorithm needs to decide if it matches a landmark from the set of all Landmarks L of the navigation map, thus forming a mapping:

$$\text{ident}: D \to L \cup \{\emptyset\} \tag{9}$$

The target set of the mapping contains the empty element to allow rejection of false-positive detections. Usually, identification is performed for every single detection without consideration of the other detections. Thus, it is possible that the identification process associates two detections with the same landmark, violating the *mutual exclusion principle in data association* [13]. Depending on the robustness of the employed localization algorithm, measures need to be taken to prevent this kind of error. These measures are usually computationally expensive, and the exclusion principle is thus often not enforced.
To create the mapping, the localization algorithm utilizes the measured and/or inferred data associated with each detection, that is, detection features. These features are general positional information like distance, bearing and orientation in relation to the robots local coordinates, and landmark-specific details that depend on the application scenario. Examples for this are height and radius for rocks or shape parameters for craters. Depending on the landmark type, available sensors and the landmark detection algorithm, some of the features might not be provided. For example, it is not possible to calculate the height of a rock using a horizontally-mounted 2D laser scanner.
Finding the most probable match for a landmark detection is achieved in two steps. First, we determine a subset $L_{\text{candidate}} \subseteq L$ of candidate landmarks:

- Initialize $L_{\text{candidate}} = L$.
- If positional features and a robot pose estimate are available, they can be combined to formulate geometric restrictions for possible landmark poses (see Figure 2). Any landmarks

which violate the geometric constraints are excluded from the candidate set.
- All landmarks where the difference between landmark feature value and corresponding detection feature value exceeds a threshold are excluded.

Second, we calculate a distance measure to find the best matching landmark from the candidate set:

$$\text{match}(d \in D) = \min_{l \in L_{\text{candidate}}} \text{dist}(d, l) \quad (10)$$

$$\text{dist}(d, l) = \sum_{\text{Feature f}} \left(\alpha_{\text{f}}(\text{f}_{\text{d}} - \text{f}_{\text{l}})\right)^2 \quad (11)$$

The feature weights α_{f} are used to scale the feature difference values according to their importance and uncertainties of the observation model. If the candidate set is empty or the minimum distance is above a threshold, the detection is rejected.

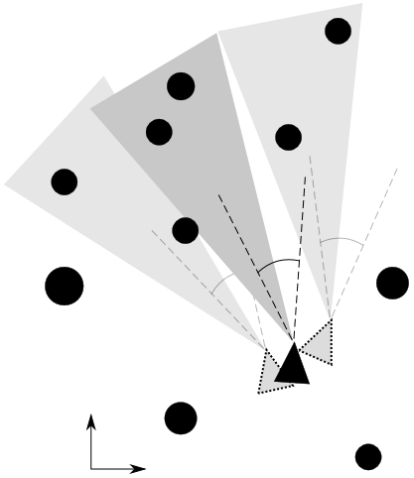

Figure 2: Selection of candidate landmarks for landmark identification using a known robot pose (black triangle) and a bearing-only measurement with bearing uncertainty (large grey triangle). Uncertainty in the robots position and orientation (dotted triangles) increase the amount of landmarks that need to be considered.

Semantic navigation maps enhance the landmark identification process: We can further reduce the landmark candidate set to include only landmarks of the type that matches the detection type. Also, the comprehensible specific class features facilitate modeling the feature difference thresholds and weights.

4.2. Using Semantic Information for Particle Filter Localization

A particle filter models the probability distribution of the robot as a set of individual robot pose estimates called particles. In each step, the algorithm updates each particle's weight to represent the conditional probability of the current observations given the particle's pose, with higher weight indicating higher probabilities [14].
To achieve this, the algorithm performs the landmark identification described above once for each particle, using the particle hypothesis as source for the transformation of the local positional features of the detection.
In this algorithm, we can make use of semantic quality data to improve the calculation of the particle weight w_i from the previously calculated match distance measures of each matched landmark. For each particle, we first calculate the total error e_i as a weighted sum of the matching errors, using the corresponding landmark's quality q_l as weight. We then use the total error to calculate the normalized positive weight.

$$e_i = \sum_{\text{Detection } d} \text{match}(d) q_l \quad (12)$$

$$e_{max} = \max_{Particle\ p} e_p \quad (13)$$

$$\text{w}_{\text{i}} = \frac{-\text{e}_i + \text{e}_{\text{max}}}{\text{e}_{\text{max}}} \quad (14)$$

Without semantic information, all detections have the same amount of influence on the particle weight. With our approach, we make sure that landmarks with a low quality rating (indicating high uncertainty regarding the existence and position of this landmark) have a lower influence on the particle weight.

4.3. Semantic Information for Kalman Filters

Similar to the approach for particle filters described above, semantic information can be utilized in localization algorithms based on Extended or Unscented Kalman Filters (EKF and UKF, see [15] and [16]). For each landmark measurement, these algorithms calculate:

- A vector called *innovation v*, which describes the difference between the actual and the expected measurement (given the current state estimate x_{t}).
- The Kalman gain matrix *K* which describes the relations between the current state covariance P_{t} and the measurement covariance P_{zz}.

The Kalman update equations use the innovation and the Kalman gain to determine the new state and state covariance:

$$x_{\text{t}} = x_{\text{t-1}} + Kv \quad (15)$$

$$P_{\text{t}} = P_{\text{t-1}} - KP_{zz}K^{\text{T}} \quad (16)$$

Using the semantic information, we model a landmark-dependent measurement model that increases the measurement covariance for landmarks with a low

quality rating. This decreases the influence of such observations, leading to a more robust localization behavior.

4.4. Semantic Information in SLAM

Localization algorithms operate on existing, usually unchanging navigation maps. In contrast, SLAM algorithms maintain a changing estimated model of their surrounding environment. Existing landmarks are updated, and new landmarks are added as the robot detects them.

Classic 2D-SLAM algorithms as described in [13] track positional uncertainty for each landmark. The uncertainty is expressed as a 2x2 covariance matrix. The authors of [13] recommend tracking the existence probability of each landmark by means of an *evidence counter*, as well as using a signature value or signature vector to disambiguate landmarks. Our semantic data perfectly fits these requirements: The landmark quality represents the existence probability, and the type-specific landmark features create the signature vectors for disambiguation. The initial generation of the state vector and state covariance matrix are straightforward and require no additional map annotations. Further, the semantic landmark quality allows us to use a landmark-dependent measurement model as in standard localization without mapping (see 4.3).

5. APPLICATION

We implemented the semantic map generation and localization as a modular localization framework as shown in Figure 3. The framework is integrated in a virtual robotics testbed featuring sensor simulation, rigid body dynamics, 3D visualization, and data logging and playback. The simulated sensors provide perfect measurement data which can optionally be modified by sensor error models. The testbed enables us to run repeatable simulations with the same input data. Ground truth data from the simulator can be used to perform quantitative evaluation of the detection and localization algorithms. Optionally,

As can be seen in Figure 3, the modular structure allows us to experiment with different sensors, in-flight and rover landmark detectors, and localization algorithms without changing the map structure or other components. Each localization algorithm uses the semantic information from the shared navigation map representation.

Further, we can change rover models and virtual environments to evaluate how a specific combination of rover model, sensor suite and processing algorithms performs in different scenarios.

Our current virtual test environment (shown in Figure 4) is a mars-like terrain with mountains, craters and rocks. We simulate the landing phase of a skycrane/rover combination, followed by an exploration phase. Our robot model is similar to the MSL rover “Curiosity”. As shown in the rightmost image of Figure 4, we have added a simulated 2D horizontal laser scanner at the rover arm, so that we can use both stereo data and laser scanners as input sources for the rover-based landmark detectors.

In the scope of the research project SELOK, we apply the concept of semantic navigation maps in two

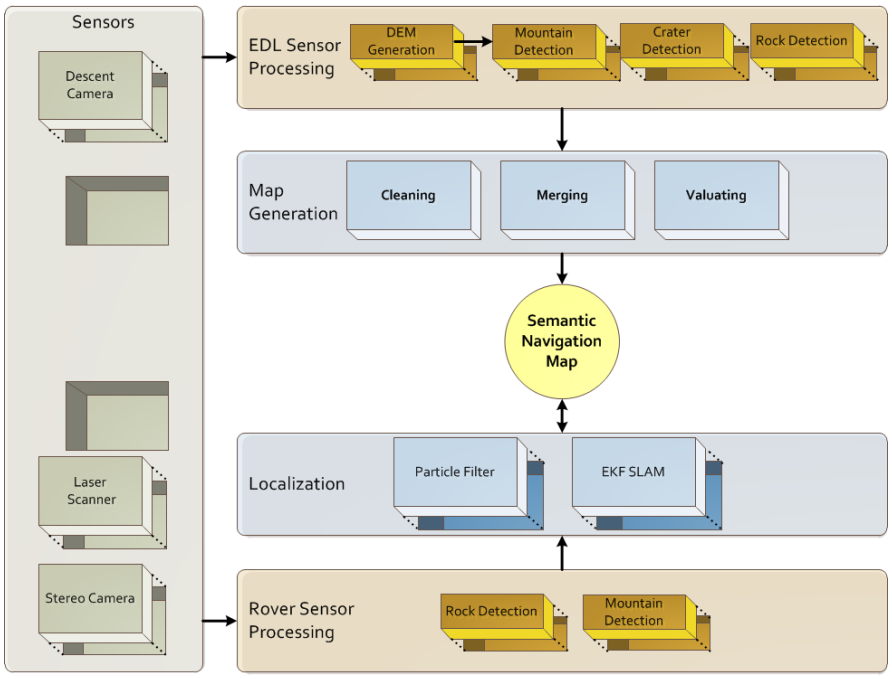

Figure 3: Semantic navigation map generation and localization in our modular localization framework

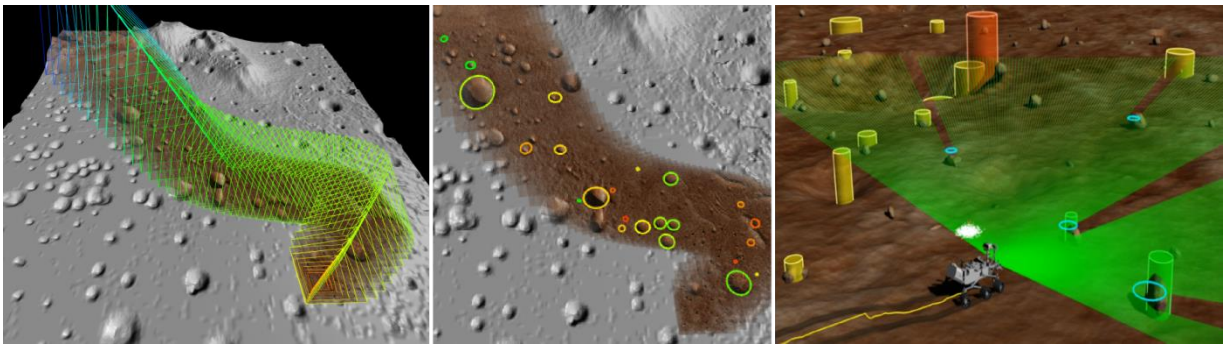

Figure 4: Scenes from our virtual testbed. Left: Landing trajectory and images projected on a DEM. Center: Crater detection and evaluation. Right: Exploration and localization with rover using the detected landmarks.

different application scenarios: Next to the planetary exploration scenario described above, the other scenario is the localization of harvesting machines in forests. In this scenario, we can evaluate our algorithms with real data in addition to simulated data.

The navigation map contains tree landmarks and is generated from airborne remote sensing data, similar to the map generation process during the EDL phase of a planetary exploration mission. We detect tree landmarks and estimate terrain shape with the methods detailed in [17] and as shown in Figure 5. The map generation process calculates the landmark positions and qualities, and approximates tree diameters from the tree height measurements. Similar to rock size and height, the tree diameter is a landmark-type specific feature value that enhances landmark identification.

To detect the landmarks during operation, the harvester has two horizontal 180° laser scanners on the cabin doors. A tree detector algorithm finds half-cylinder-like patterns in the laser echo profiles and calculates the features' distance and bearing to each pattern, as well as the diameter. The localization module provides visual support for the human operator, enables the generation of geo-referenced tree data, and allows tracking of machine movement patterns.

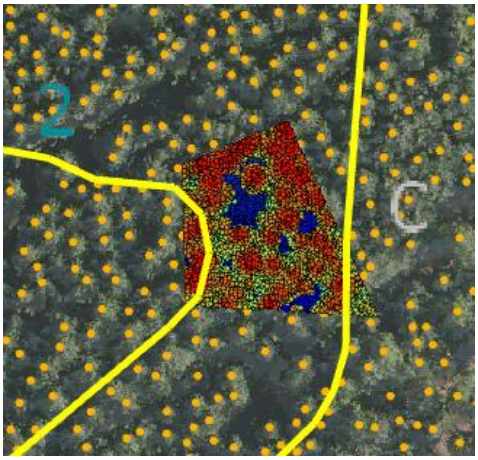

Figure 5: Semantic navigation maps for forested areas. Tree landmarks (orange dots) are generated from airborne images and laser range data (center).

6. FUTURE WORK

We plan to use the semantic map concept for the evaluation of localization and SLAM algorithms. To this end, we will implement several different algorithms that use the shared map representation.

Further, we want to perform mobile robot localization in other application environments like indoors or urban areas. With the map concept and localization algorithms already implemented, this adaption can be performed by defining the appropriate landmark types for the target application, and implementing new landmark detectors for the sensors that are available in the application context.

Finally, we plan to develop a navigation framework which utilizes the semantic navigation maps and the results from the localization algorithms. The comprehensible object representation in our map allows us to develop a variety of path planning and obstacle avoidance modules. Also, semantic information could enable a path planning algorithm to prefer a path which keeps a sufficient number of landmarks with high observability rating in sensor range at all times over a path that does not.

7. CONCLUSION

We have presented a multi-purpose map concept that extends the standard landmark-based map representation. We have shown how the semantic navigation map is generated from descent and landing imagery in a robotic exploration mission, and how the concept can be adapted to other application scenarios. Our map representation is integrated into a virtual robotics testbed and is used by different localization algorithms.

ACKNOWLEDGMENTS

The projects FastMap and SELOK are funded by the German Aerospace Center (DLR) with funds provided by the Federal Ministry of Economics and Technology (BMWi) under grant number [50 RA 1034] for FastMap and [50 RA 0911] for SELOK.

REFERENCES

1. Filliat, D & Meyer, J.-A. (2003). Map-based Navigation in Mobile Robots. A Review of Localization Strategies. In *Cognitive Systems Research, Vol. 4*, Issue 4, pp243-282.
2. Montemerlo, M., Thrun, S., Koller, D. & Wegbreit, B. (2002). FastSLAM: A Factored Solution to the Simultaneous Localization and Mapping Problem. In *Proc. AAAI National Conference on Artificial Intelligence*, pp593–598.
3. Betke, M. & Gurvits, K. (1994). Mobile Robot Localization using Landmarks. In *Proc. IEEE International Conference on Robotics and Automation (ICRA-9)*, Vol. 2, IEEE Press, pp135-142.
4. Milstein, A. (2008). Occupancy Grid Maps for Localization and Mapping. In *Motion Planning*, Xing-Jian Jing (Ed.), InTech, pp381-408.
5. Roßmann, J., Schlette, C., Emde, M., Sondermann, B., (2010). Discussion of a Self-Localization and Navigation Unit for Mobile Robots in Extraterrestrial Environments. In *Proc 10th International Symposium on Artificial Intelligence,Robotics and Automation in Space (i-SAIRAS 2010)*, Sapporo, Japan.
6. Wiens, R., et al. (2005). ChemCam Science Objectives for the Mars Science Laboratory (MSL) Rover. In *Proc. Lunar and Planetary Science, 36*, pp1580-1581.
7. Cheng, Y., Johnson, A. E., Matthies, L. H., & Olson, C. F. (2003). Optical Landmark Detection for Spacecraft Navigation. In *13th Annual AAS/AIAA Space Flight Mechanics Meeting.*
8. Tompkins, P., Stentz, A., & Wettergreen, D. (2004). Global Path Planning for Mars Rover Exploration. In *Aerospace Conference, 2004. Proceedings. 2004 IEEE*.
9. Cozman, F., & Krotkov, E. (1998). Automatic Mountain Detection and Pose Estimation for Teleoperation of Lunar Rovers. In *Experimental Robotics V* (pp. 207-215). Springer Berlin Heidelberg.
10. Mannel, C., Müller, H. & Esser, D. (2012). Generating Semi Global Elevation Maps from Planetary Descent Imagery using Bundle Adjustment. In *Proc. 11th International Symposium on Artificial Intelligence, Robotics and Automation in Space (i-SAIRAS 2012)*, Turin, Italy.
11. Huertas, A., Cheng, Y., & Madison, R. (2006). Passive Imaging Based Multi-cue Hazard Detection for Spacecraft Safe Landing. In *Aerospace Conference 2006*, IEEE.
12. Roßmann, J. & Jochmann, G. (2012). A Localization Framework for the Planning, Analysis and Execution of Mobile Robot Missions. In *Proc. 11th International Symposium on Artificial Intelligence, Robotics and Automation in Space (i-SAIRAS 2012)*, Turin, Italy.
13. Thrun, S., Burgard, W. & Fox, D. (2005). *Probabilistic Robotics*. The MIT Press.
14. Thrun, S. (2002). Particle Filters in Robotics, In *Proc 17th Annual Conference on Uncertainty in AI (UAI)*, Morgan Kaufmann Publishers Inc, pp511-518
15. Julier, S., Uhlmann, J. (1997). New Extension of the Kalman Filter to Nonlinear Systems. In *Proc. Signal Processing, Sensor Fusion, and Target Recognition 6*, Orlando.
16. Wan, E., Merwe, R. (2001). The Unscented Kalman Filter. In *Kalman Filtering and Neural Networks*, Wiley, pp221-280.
17. Bücken, A., Roßmann, J. (2013). From the Volumetric Algorithm for Single-Tree Delineation Towards a Fully-Automated Process for the Generation of "Virtual Forests". In *Pouliot, J./Daniel, S./Hubert, F./Zamyadi, A.: "Progress and New Trends in 3D Geoinformation Sciences*", Lecture Notes in Geoinformation and Cartography, Springer, pp79-99.